# Structural and stratigraphic evolution of extensional oceanic arcs

Benjamin N. Fackler-Adams
Cathy J. Busby
Department of Geological Sciences, University of California, Santa Barbara, California 93106

**ABSTRACT**

**We present a general model for the structural and stratigraphic evolution of extensional oceanic arcs, combining published data from modern oceanic arcs with our outcrop data from a Cretaceous oceanic arc in Baja California. Thirty lithofacies building blocks are assembled into architectural models for two phases of evolution. Phase I is characterized by intermediate to silicic explosive and effusive volcanism, culminating in caldera-forming silicic ignimbrite eruptions. This represents an extensional island arc, with the onset of arc rifting being recorded in the climactic caldera-forming eruptions. Phase II is characterized by mafic effusive and hydroclastic rocks and widespread dike swarms, and it records rifting of the arc. The cycle of arc extension followed by arc rifting reflects the episodicity of rifting in arc-backarc systems, which appears to recur on 10–15 m.y. time scales.**

## INTRODUCTION

The strain regime in the upper plate of arc-trench systems may be extensional, neutral, or compressional (Dewey, 1980). A strong positive correlation exists between the duration of subduction and the strain regime in the overriding plate (Jarrard, 1989). Modern Earth is strongly biased toward compressional arcs, because most modern subduction zones have been extant for at least 65 m.y. (Jarrard, 1986). Therefore, studies of ancient convergent margins are critical to understanding of extensional arcs.

Recent years have seen major advances in understanding of the tectonic, volcanic, and sedimentary character of modern oceanic arcs through the use of submersible studies, dredging, coring, and sonar, magnetic, and seismic surveys (e.g., Bloomer et al., 1989; Taylor et al., 1990, 1991; Nishimura et al., 1992; Taylor, 1992; Klaus et al. 1992; Clift et al., 1995). These studies give a largely two-dimensional view of oceanic arcs. This paper reports on a detailed three-dimensional outcrop study of the unusually well preserved and well-exposed Cretaceous Alisitos arc (Fig. 1). The Alisitos arc lies in the western wall of the Peninsular Ranges batholith (for more on the geologic setting, see references in Busby et al., 1998). The segment described here contains only very small-displacement postdepositional faults, and subgreenschist metamorphism allows recognition of primary microtextures.

Detailed (1:10 000 scale) mapping of a 50 × 30 km segment of the Alisitos arc (Fig. 1) has documented an emergent (subaerial) stratovolcano flanked by marine basins to the present-day north and south (Fackler-Adams, 1997). The southern marine basin is a volcano-bounded basin (sensu Smith and Landis, 1995) where strata accumulated in shallow- to deep-water environments between constructive volcanic centers (Fig. 2A). The northern marine basin, in contrast, is a fault-bounded or hybrid basin (fault-bounded basin hereafter), which was downthrown into deep water relative to the stratovolcano along a fault zone. This fault zone may have controlled the siting of the stratovolcano, and the boundary of an 8-km-wide caldera that formed at its summit (Fig. 2A).

Two distinct evolutionary phases of the Alisitos arc terrane are recognized (Figs. 1 and 2). We predict that these phases will be recognized in most modern and ancient oceanic arc terranes. Phase I is characterized by intermediate to silicic explosive and effusive volcanism, culminating in caldera-forming silicic ignimbrite eruptions (Fig. 2A). Phase II is characterized by mafic effusive and hydroclastic volcanism and injection of dike swarms. We interpret phase I to represent an extensional island arc; the onset of arc rifting being recorded in the climactic caldera-forming eruption. Phase II records rifting of the arc. The phase I–phase II cycle reflects the 10–15 m.y. episodicity of rifting in arc-backarc systems resulting from progressive migration of the back-arc spreading center away from the trench (Taylor and Karner, 1983).

The purpose of this paper is to define a model for extensional (phase I) and rift (phase II) phases in the structural and stratigraphic evolution of extensional oceanic arcs (Fig. 2). This model combines our field data with recently

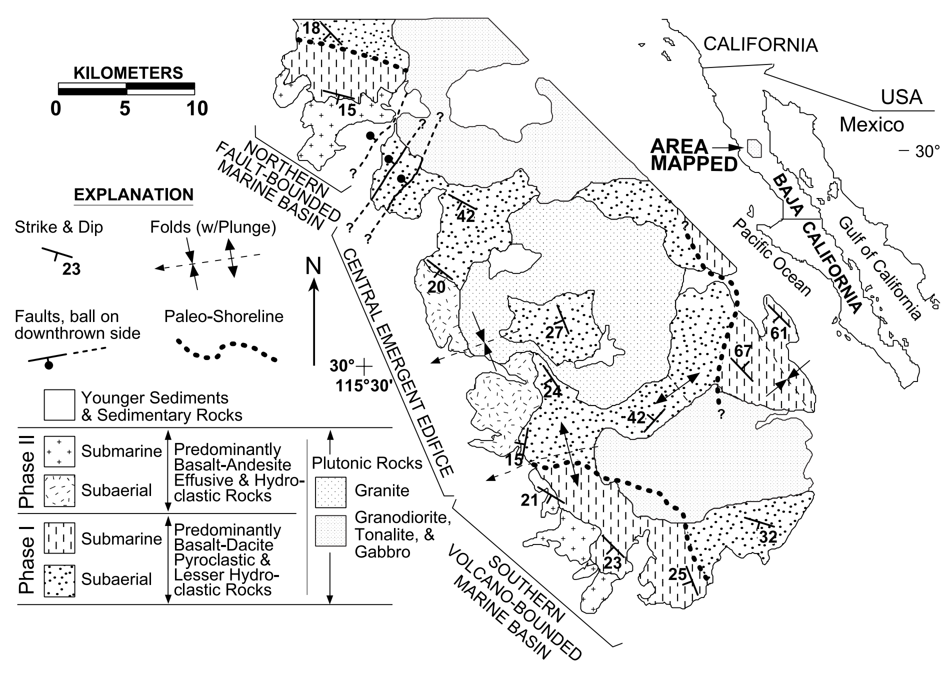


**Figure 1. Generalized geologic map of a 50 × 30 km segment of Cretaceous Alisitos arc, Baja California, Mexico.**

published oceanographic data, and uses 30 lithofacies as its fundamental building blocks.

## OCEANIC ARC LITHOFACIES

The segment of the Alisitos arc described here forms a section ~3000 m thick, with contemporaneous intrusive rocks (Figs 1 and 2). Because facies changes in arc terranes are typically too rapid to allow establishment of formations and members, lithofacies mapping and analysis are employed. More detailed petrographic and textural characteristics of these lithofacies are available in Fackler-Adams (1997). Lithofacies descriptions proceed from least to most explosive volcanism, and from mafic to felsic compositions within those categories, followed by lithofacies formed by remobilized eruptive products and by non-volcanic sediments. These 30 lithofacies were mapped individually on a scale of 1:100 00 (Fackler-Adams, 1997); here we present generalized map units that show the grouping of these lithofacies during the two phases of arc evolution (Fig. 2).

### Lithofacies in both Subaerial and Marine Environments

Effusive volcanic lithofacies include coherent lava flows, as well as flow breccias formed by autobrecciation; these are basaltic to andesitic in composition. Fire-fountain agglomerate consists of accumulations of fluidal basaltic or andesitic clasts (spatter). Highly viscous silicic lava flows are mainly thick, coarse-grained dome breccias.

Hydroclastic breccias are massive, clast-supported accumulations of glassy cuspate blocks produced by quench fragmentation of lava flows. Hydroclastic tuffs and lapilli tuffs are massive or stratified accumulations that have blocky and cuspate shards, and form by phreatomagmatic eruptions and quench fragmentation of lava flows. Polymict accumulations of altered volcanic rock fragments can result from phreatic explosions.

Pyroclastic rocks all show evidence of explosive fragmentation by expansion of magmatic volatiles. Pyroclastic fallout forms by widespread settling of pyroclasts through air or water, and most commonly consists of well-sorted, well-stratified tuff and lapilli-tuff beds that mantle topography. Pyroclastic flows are hot, gas-fluidized flows that are more concentrated than pyroclastic surges (discussed in the following section). Pyroclastic flows form four types of poorly sorted, generally massive deposits with ashy matrix. (1) Block-and-ash flows are mafic to silicic in composition, and have poorly vesiculated blocks generated by lava flow-front or dome collapse. (2) Scoria-and-ash flows are mafic to intermediate in composition, have moderately vesiculated lapilli, and result from explosive eruptions. (3) Ignimbrites are intermediate to felsic in composition, have highly vesiculated clasts (pumice), and result from explosive eruptions. (4) Welded ignimbrite shows vitroplastic flattening of shards indicative of very high emplacement temperatures, and are present in both marine and subaerial environments.

Remobilized (mass wasting) deposits are commonly polylithic, largely massive, and most commonly emplaced cold. Lithofacies include: (1) debris-flow deposits (or lahars), which are matrix-supported beds as much as a few tens of meters thick, and (2) debris-avalanche deposits, which are tens to hundreds of meters thick and contain blocks up to hundreds of meters in size.

There are intrusions throughout both the subaerial and marine parts of the arc that range from microcrystalline to coarsely porphyritic and holocrystalline textures.

### Lithofacies only in Subaerial Environments

Of the primary volcanic rock types, only pyroclastic surge appears to be restricted to the subaerial environment. It produces a moderately to well-sorted, well-stratified and cross-stratified deposit. Unlike pyroclastic flows, pyroclastic surges are too dilute and turbulent to flow beneath water and remain gas-fluidized.

All the other lithofacies restricted to subaerial environments reflect the work of running water. Hyperconcentrated flood flows are common in volcanic settings, where sediment supply is episodically very high; these are distinguished from more dilute fluvial flow deposits by a lack of cross-stratification and a more massive character (Smith, 1991). Both fluvial and hyperconcentrated flood flow lithofacies can be subdivided into gravelly and sandy types.

Paleosol horizons are rarer and less-well developed than they are in most other tectonic settings, because subsidence rates in extensional arcs are high, leading to rapid burial of deposits.

### Lithofacies only in Marine Environments

Primary volcanic lithofacies include mafic pillow lava and pillow breccia, as well as silicic fire-fountain agglomerate. The latter are enigmatic because silicic lavas are commonly too viscous to produce spatter accumulations. They appear to be restricted to deep-water sections in the Alisitos arc. The fluidal nature of the lavas may result from hydrostatic pressure suppressing volatile exsolution (Cas, 1978), or alternatively, might result from high-temperature fissure eruptions (McCurray et al., 1997).

Pyroclastic deposits showing features typical of low-and high-density turbidity current deposits are referred to as the tuff turbidite lithofacies. These may be eruption fed or may represent remobilized pyroclastic detritus, but liquid water, not gas, forms the interstitial fluid. We subdivide the tuff turbidite lithofacies into coarse-grained tuff turbidites, massive tuff turbidites, and laminated tuff turbidites. These are analogous to the gravelly high-density turbidites, sandy high-density turbidites, and low-density turbidity currents of Lowe (1982), respectively. The laminated tuff turbidites form a continuum with tuffaceous siltstone and mudstone composed of vitric clasts, crystals, volcanic rock fragments, and lime mud. These record dilute turbidity current and suspension sedimentation of fine-grained bioclastic and volcaniclastic detritus.

Subrounded, relatively well-sorted, clast-supported accumulations of cobbles and pebbles are interpreted as beach conglomerate deposits. This lithofacies is limited in extent, due to steep volcano flanks, and is texturally immature relative to beach deposits in other tectonic settings, due to high sediment supply and rapid burial.

Biogenic sedimentary rocks in the Alisitos arc will not necessarily resemble those of other arcs, because reef-forming organisms vary with geologic age and paleolatitude. In the Alisitos arc, rudists built bioherms in the photic zone, and bioclastic turbidites extended into deep water.

## PHASE I: EXTENSIONAL OCEANIC ARC

Figure 2A is a reconstructed cross section of part of the Alisitos arc as it was beginning to “unzip,” by analogy with the Izu-Bonin arc-backarc system (e.g., Taylor et al., 1990; Clift et al., 1995; Arculus et al., 1995). Rift propagation in modern arcs takes more than 5 m.y. (Tamaki et al., 1992; Taylor, 1992). In the Izu-Bonin arc, rifting and the resultant change in stress regime produce silicic calderas (Gill et al., 1992); these provide voluminous dacitic pyroclastic debris that dominates the stratigraphic record (Nishimura et al., 1992). Stratigraphic evidence of a caldera-forming eruption on the stratovolcano occurs across the 50-km-long mapped segment of the Alisitos arc.

Caldera collapse on the stratovolcano ponded welded dacite ignimbrite to a thickness of at least 3 km (tuff of Aguajito, Fig. 2A). The subaerial outflow facies is as thick as 300 m, and densely welded even where only a few meters thick. Outflow ignimbrite traversed a dacite dome complex to the south, and entered the volcano-bounded marine basin (subaqueous tuff of Aguajito, Fig. 2A), where it is not welded, but shows evidence of heat retention in some flow units (Fackler-Adams, 1997). In the northern fault-bounded basin, the tuff of Aguajito occurs as blocks, as much as 150 m across, emplaced as part of a debris-avalanche deposit shed into deep water from the faulted basin margin (Fig. 2A). These blocks were hot enough to deform plastically, and to form peperite with the substrate and debris-avalanche matrix. The debris avalanche was probably triggered by injection of feeder dikes along the fault zone during the caldera-forming eruption (Fig. 2A). Dike injections are known to produce the largest sector collapses on Earth (Moore et al., 1994). This might explain why the debris-avalanche deposit is thicker and larger than many generated by sector collapse of stratovolcanoes, although it is substantially

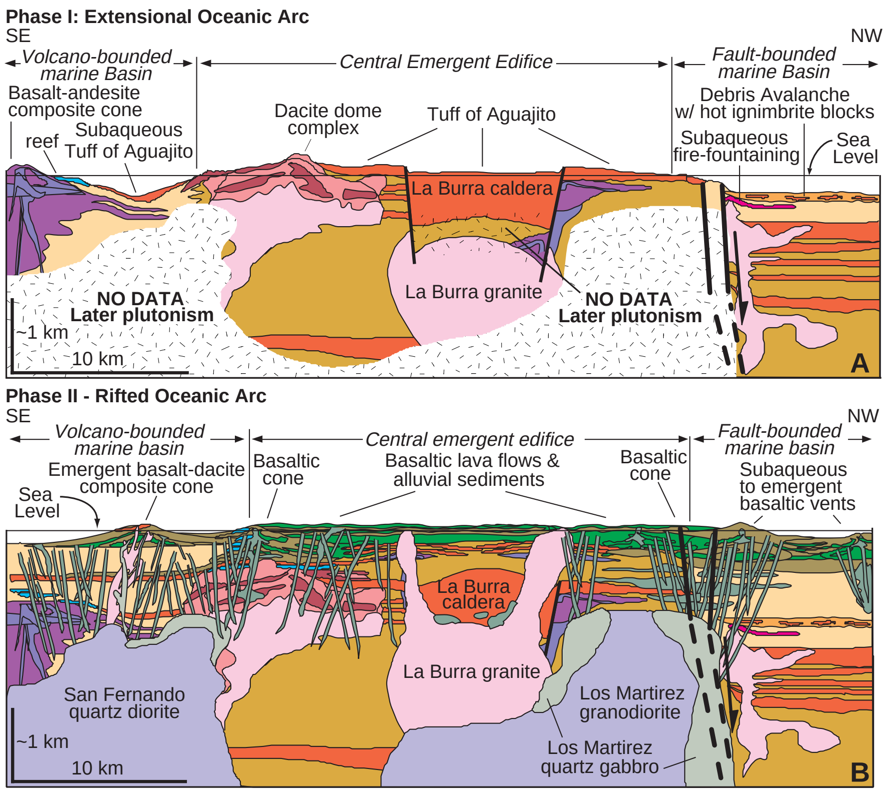


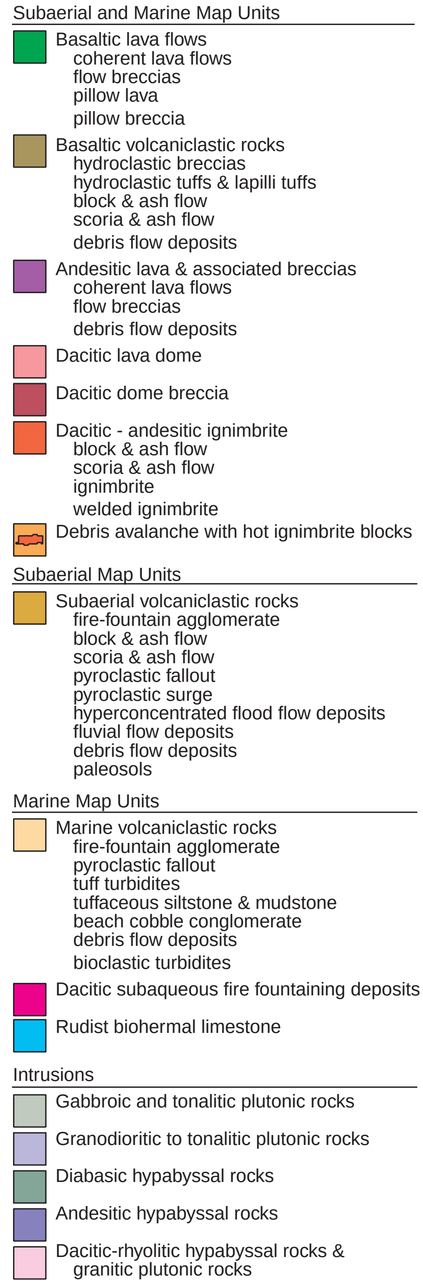


**Figure 2. Schematic cross sections of portion of Alisitos arc mapped in Figure 1, depicting evolutionary phases of extensional oceanic arcs. A: Phase I during extension of the oceanic arc. B: Phase II after onset of arc rifting.**

smaller than deposits generated by collapse of giant hot spot volcanoes (Siebert et al., 1987).

The southern volcano- and northern fault-bounded marine basins flanking the stratovolcano have contrasting characteristics. (1) Tuff turbidites are more common than pyroclastic flow deposits in the fault-bounded basin than the volcano-bounded basin. This is because pyroclastic flows mixed more completely with water when they traversed the rugged, fault-controlled margin of the northern basin. (2) Volcanism within the volcano-bounded basin was limited to small-volume nonexplosive eruptions at a central vent. In contrast, the fault zone at the margin of the basin plumbed larger volumes of magma to the surface, producing silicic pyroclastic calderas and dacite fire fountain agglomerate. (3) Slumping and other mass-wasting events were rare and small-scale in the volcano-bounded basin relative to the fault-bounded basin, where topography was steeper and seismicity more common. (4) Rudist bioherms and associated bioclastic turbidites are well developed in the volcano-bounded basin, and absent in the fault-bounded basin because the steeper, unstable slopes of the fault-bounded basin were unfavorable for the development of bioherms.

## PHASE II: RIFTED OCEANIC ARC

Figure 2B is a reconstructed cross section of the Alisitos arc segment during eruption of rift basalts and emplacement of associated dike swarms. The generally sharp contact between phase I and phase II strata, and the predominance of lavas over fluvial or marine volcaniclastic rocks indicates that the onset of rift basalt volcanism was abrupt and voluminous. As a result, the central edifice was transformed from a stratovolcano with a summit caldera into a basalt lava plateau fringed by small basaltic cones (Fig. 2B).

The southern volcano-bounded and northern fault-bounded basins differed in two important ways during arc rifting. (1) Volcanism in the volcano-bounded basin was centered at one vent, which evolved andesitic and dacitic magmas, whereas volcanism in the fault-bounded basin was noncentralized, and entirely mafic. This suggests that faulting of the northern basin provided multiple unhindered conduits for the ascent of mafic magma. (2) The first construction of an emergent cone within the volcano-bounded basin occurred during phase 2, while vents remained submerged in the fault-bounded basin. This indicates that subsidence in the fault-bounded basin outpaced rapid aggradation of basaltic lavas and volcaniclastic rocks during arc rifting.

## DISCUSSION

Subsidence rates inferred for the Alisitos arc agree with those reported for rifts in other tectonic settings (Busby and Ingersoll, 1995). Photic-zone rudist reefs of Aptian–Albian age occur along the margins of the volcano-bounded basin throughout most of the 3-km-thick section, indicating that sediment-accumulation rates approximated subsidence rates. It is not clear if the entire Aptian–Albian (~20 m.y.) is represented. If so, a minimum subsidence rate of 150 m/m.y. occurred. If the Alisitos arc had a life span more typical of modern extensional oceanic arcs (10–15 m.y.), a subsidence rate of 200–300 m/m.y. or greater is required. Our zircon geochronology in progress supports this higher rate. In either case, the subsidence rate is typical of rift settings, and is too rapid for nontectonic causes of subsidence (e.g., thermal subsidence, sediment loading).

Our regional studies in Baja California indicate that the Alisitos arc formed under an extensional strain regime; however, while normal faults were pervasive in the forearc region (Busby et al., 1998), they appear to be restricted to a single fault zone in the 50 × 30 km arc segment we have mapped (Figs. 1 and 2). This is not surprising, because Taylor (1992) showed that normal faults in the modern Izu-Bonin arc are best developed between major volcanic centers at which extension is largely accommodated by intrusions, and our study is of a major center in the Alisitos arc. By analogy with the Izu-Bonin arc, we predict that segments of the Alisitos arc that lie between major volcanic centers will show more pervasive faulting. In more dismembered ancient arcs, it may be difficult to recognize extension. This is because more pervasively faulted intervolcano segments cannot be easily distinguished from forearc or backarc basins, because they lack the hypabyssal intrusions and vent-proximal features that are used to recognize ancient arcs.

In conclusion, we propose that the two phases of evolution recorded by the Alisitos arc are representative of the structural and stratigraphic evolution of extensional oceanic arcs.


## ACKNOWLEDGMENTS

This research was supported by National Science Foundation Grant EAR 93-04130 to C. Busby. Insightful reviews by Richard Arculus and Brian Taylor improved the manuscript.


## REFERENCES CITED


Arculus, R. J., Gill, J. B., Cambray, H., Chen, W., and Stern, R. J., 1995, Geochemical evolution of arc systems in the western Pacific: The ash and turbidite record recovered by drilling, *in* Taylor, B., and Natland, J., eds., Active margins and marginal basins of the western Pacific: American Geophysical Union Monograph 88, p. 45–65.

Bloomer, S., Stern, R., and Smoot, C., 1989, Physical volcanology of the submarine Mariana and Volcano Arcs: Bulletin of Volcanology, v. 51, p. 210–224.

Busby, C. J., and Ingersoll, R. V., eds., 1995, Tectonics of sedimentary basins: Blackwell Science: Cambridge, 579 p.

Busby, C. J., Smith, D. P., Morris, W., and Fackler-Adams, B. N., 1998, Evolutionary model for convergent margins facing large ocean basins: Mesozoic Baja California, Mexico: Geology, v. 26, p. 227–230.

Cas, R. A. F., 1978, Silicic lavas in Paleozoic flysch-like deposits in New South Wales, Australia: Behavior of deep subaqueous silicic flows: Geological Society of America Bulletin, v. 89, p. 1708–1714.

Clift, P. D., and ODP Leg 135 Scientific Party, 1995, Volcanism and sedimentation in a rifting island-arc terrane: An example from Tonga, southwest Pacific, *in* Smellie, J. L., ed., Volcanism associated with extension at consuming plate margins: Geological Society London Special Publication 81, p. 29–51.

Dewey, J. F., 1980, Episodicity, sequence, and style at convergent plate boundaries, *in* Strangway, D. W., ed., The continental crust and its mineral deposits: Geological Association of Canada Special Paper 20, p. 553–573.

Fackler-Adams, B. N., 1997, Volcanic and sedimentary facies, processes, and tectonics of intra-arc basins: Jurassic continental arc of California and Cretaceous oceanic arc of Baja California, [Ph.D. thesis]: Santa Barbara, University of California, 248 p.

Gill, J., Seales, C., Thompson, P., Hochstaedter, A., and Dunlap, C., 1992, Petrology and geochemistry of Pliocene-Pleistocene volcanic rocks from the Izu Arc, Leg 126, *in* Taylor, B, Fujioka, K., Janecek, T., and Langmuir, C., eds., Proceedings of the Ocean Drilling Program, Scientific results, Bonin Arc-Trench System, Leg 126, Sites 787–793, Volume 126: College Station, Texas, Ocean Drilling Program, p. 383–404.

Jarrard, R. D., 1986, Relations among subduction parameters: Reviews of Geophysics, v. 24, p. 217–284.

Klaus, A., Taylor, B., Moore, G., MacKay, M., Brown, G. R., Okamura, Y., and Murakami, F., 1992, Structural and stratigraphic evolution of the Sumisu Rift, Izu-Bonin arc, *in* Taylor, B, Fujioka, K., Janecek, T., and Langmuir, C., eds., Proceedings of the Ocean Drilling Program, Scientific results, Bonin Arc-Trench System, Leg 126, Sites 787–793, Volume 126: College Station, Texas, Ocean Drilling Program, p. 555–573.

Lowe, D. R., 1982, Sediment gravity flows II: Depositional models with special reference of the deposits of high density turbidity currents: Journal of Sedimentary Petrology, v. 52, p. 279–297.

McCurray, M., Bonnichsen, B., White, C., Godchaux, M., and Hughes, S., 1997, Bimodal basalt-rhyolite magmatism in the central and western Snake River Plain, Idaho and Oregon: Brigham Young University Geologic Studies 1997, v. 42, p. 381–422.

Moore, J. G., Normark, W. R., and Holcomb, R. T., 1994, Giant Hawaiian underwater landslides, Science, v. 264, p. 46–47.

Nishimura, A., Rodolfo, K., Koizumi, A., Gill, J. B., and Fujioka, K., 1992, Episodic deposition of Pliocene-Pleistocene pumice deposits of the Izu-Bonin Arc, *in* Taylor, B., Fujioka, K., Janecek, T., and Langmuir, C., eds., Proceedings of the Ocean Drilling Program, Scientific results, Bonin Arc-Trench System, Leg 126, Sites 787–793, Volume 126: College Station, Texas, Ocean Drilling Program, p. 3–21.

Siebert, L., Glicken H. X., and Ui, T., 1987, Volcanic hazards from Bezmianny- and Bandai-type eruptions; Bulletin of Volcanology, v. 49, p. 435–459.

Smith, G. A., 1991, Facies sequences and geometries in continental volcaniclastic sequences, *in* Fisher, R. V., and Smith, G. A., eds., Sedimentation in volcanic settings: SEPM (Society for Sedimentary Geology) Special Publication 45, p. 109–122.

Smith, G. A., and Landis, C. A., 1995, Intra-arc Basins, *in* Busby, C. J., and Ingersoll, R. V., eds., Tectonics of sedimentary basins: Cambridge, Blackwell Science, p. 263–298.

Tamaki, K., Suyehiro, K., Allan, J., Ingle, J. C., Jr., and Pisciotto, K. A., 1992, Tectonic synthesis and implications of Japan Sea ODP drilling: *in* Tamaki, K., Suyehiro, K., Allan, J., and McWilliams, M., eds., Proceedings of the Ocean Drilling Program; Scientific results; Japan Sea, Legs 127 and 128, sites 794–797, Volume 127/128: College Station, Texas, Ocean Drilling Program, p. 1333–1348.

Taylor, B., 1992, Rifting and the volcano-tectonic evolution of the Izu-Bonin-Mariana arc, *in* Taylor, B, Fujioka, K., Janecek, T., and Langmuir, C., eds., Proceedings of the Ocean Drilling Program, Scientific results, Volume 126: College Station, Texas, Ocean Drilling Program, p. 627–651.

Taylor, B., and Karner, G. D., 1983, On the evolution of marginal basins: Reviews of Geophysics and Space Physics, v. 21, no. 8, p. 1727–1741.

Taylor, B., Brown, G., Fryer, P., Gill, J. B., Hochstaedter, A. G., Hotta, H., Langmuir, C. H., Leinen, M., Nishimura, A., and Urabe, T., 1990, ALVIN-SeaBeam studies of the Sumisu Rift, Izu-Bonin Arc: Earth and Planetary Science Letters, v. 100, p. 127–147.

Taylor, B, Klaus, A., Brown, G. R., Moore, G. F., Okamura, Y., and Murakami, F., 1991, Structural development of Sumisu Rift, Izu-Bonin Arc: Journal of Geophysical Research, v. 96, p. 16113–16129.



Manuscript received January 26, 1998
Revised manuscript received May 18, 1998
Manuscript accepted May 31, 1998